Effect of process variables on formation of dynamic strain induced ultrafine ferrite during hot torsion testing

P. J. Hurley and P. D. Hodgson

Ultrafine grain sizes were produced using hot torsion testing of a 0·11C–1·68Mn–0·20Si (wt-%) steel, with ultrafine ferrite (<1 μm) nucleating intragranularly during testing by dynamic strain induced transformation. A systematic study was made of the effect of isothermal deformation temperature, strain level, strain rate, and accelerated cooling during deformation on the formation of ultrafine ferrite by this process. Decreasing the isothermal testing temperature below the Ae_3 temperature led to a greater driving force for ferrite nucleation and thus more extensive nucleation during testing; the formation of Widmanstätten ferrite prior to, or early during, deformation imposed a lower temperature limit. Increasing the strain above that where ferrite first began (0·8 at 675°C and a strain rate of 3 s^{-1}) increased the intragranular nucleation of ferrite. Strain rate appeared to have little effect on the amount of ferrite formed. However, slower strain rates led to extensive polygonisation of the ferrite formed because more time was available for ferrite recovery. Accelerated cooling during deformation followed by air cooling to room temperature led to a uniform microstructure consisting of very fine ferrite grains and fine spherical carbides located in the grain boundaries regions. Air cooling after isothermal testing led to carbide bands and a larger ferrite grain size. **MST/4873**

Dr Hurley, formerly in the Department of Materials Engineering, Monash University, Melbourne, Australia 3800, is now at the Manchester Materials Science Centre, University of Manchester & UMIST, Manchester M1 7HS, UK (peter.j.hurley@umist.ac.uk). Professor Hodgson is in the School of Engineering and Technology, Deakin University, Geelong, Victoria, Australia 3217. *Manuscript received 9 October 2000; accepted 22 January 2001.*

Introduction

It is well known that solid state phase transformations may be mechanically induced during deformation by the production of new nucleation sites (defects) by plastic strain; these are termed 'strain induced transformations'.[1] In steels, when this occurs dynamically (i.e. during deformation or in the brief period following deformation) very efficient ferrite grain refinement can be achieved.[2–4]

Priestner and de los Rios[3] were among the first to recognise that extra grain refinement may be possible in steels if the transformation could be induced during the deformation process. They studied C–Mn steel and two microalloyed steels, where extra grain refinement was observed when ferrite formed in the roll gap. Their work indicated that it was the austenite substructure that gave rise to the further grain refinement. Transgranular deformation bands were reported as the most prolific source of extra ferrite nucleation sites. Priestner later described the effect as a 'strain induced transformation'.[4] It was proposed[3] that the extra grain refinement was largely due to the absence of a delay between deformation and transformation. This effectively eliminates the possibility for recovery processes to occur within the austenite, thus enhancing the ability of deformation bands to nucleate ferrite. This idea was supported by Amin and Pickering,[5] who concluded that recovery of the dislocation substructure within deformation bands decreases the potential for ferrite nucleation on these bands. Thus it appears that the most important feature of a dynamic strain induced transformation (DSIT) is that intragranular ferrite nucleation occurs simultaneously with deformation, the nucleation having occurred before recovery has eliminated the potency of the intragranular nucleation sites.

Several workers have now produced ultrafine ferrite grain sizes (i.e. less than 2 μm) as a result of extensive intragranular nucleation of ferrite during deformation (i.e. DSIT).[6–13] However, no systematic investigation has been carried out to quantify the effect of process variables on the efficiency of DSIT as a mechanism for producing ultrafine grained steels.

In a previous paper, it was shown that ultrafine ferrite grain sizes could be achieved in low carbon steel by DSIT at the surface of specimens deformed using hot torsion testing.[14] One of the key advantages of torsion testing is that it allows individual process variables, such as temperature, strain and strain rate, to be isolated. Thus, in the present paper, a systematic evaluation of the effect of a number of process variables on the phenomenon of DSIT is made using hot torsion.

Experimental

MATERIALS AND TECHNIQUES

The composition of the steel used in the present work was Fe–0·111C–0·20Si–1·68Mn–0·022P–0·0020S–0·019Cr–0·023Mo–0·019Ni–0·027Al–0·013C (wt-%). The Ae_3 temperature of this steel was calculated to be 817°C, using the method of Kirkaldy *et al.*[15] A 75 kg vacuum cast billet was reduced in thickness by hot rolling at temperatures between 1200°C and 1000°C to 20 mm.

The hot torsion machine used in this work, which was located at BHP Research Melbourne Laboratories, has been described extensively by Weiss *et al.*[16] During testing, the entire length of specimens is enclosed in a quartz glass tube, in which a positive pressure of argon is maintained to prevent oxidation and decarburisation of the specimen. Torsion specimens (gauge length 20 mm, gauge diameter 6·7 mm) were machined from the 20 mm plate, with the axis of the torsion specimen parallel to the rolling direction of the plate. Two holes were drilled along the axis of each specimen through the shoulder to the start of the gauge length so that an N type thermocouple could be inserted

 ISSN 0267–0836

into each end of the specimen during testing to allow the temperature at the edge of the gauge length to be measured. Equivalent true stress – true strain values were calculated from the torque – twist data using the method based on the analysis by Fields and Backofen.[17,18] Following testing, metallographic examination of the torsion specimens was performed on sections cut through the centre of each specimen parallel to the axis of the specimen ($z-r$ plane) as well as on 1 mm thick slices cut tangential to the surface ($z-\theta$ plane).

TORSION SCHEDULES

Effect of deformation temperature

The aim of this set of experiments was to determine the extent of the temperature range over which intragranular ferrite nucleation could be induced during isothermal deformation for this steel. Samples were initially heated to 1250°C for 5 min to produce an austenite grain size of $\sim$200 μm, air cooled to the testing temperature, held for 10 s to allow the temperature to stabilise and then deformed to a von Mises equivalent tensile strain (hereunder referred to as strain) of 2·0 at an equivalent tensile strain rate (hereunder referred to as strain rate) of 3 s^{-1}. Testing temperatures of 825°C (above Ae_3), 750°C, 725°C, 700°C, 675°C, and 650°C were used. The samples were water quenched (within 1 s) once deformation had ceased.

Effect of strain

This series of tests were used to assess the effect of strain level on the extent of DSIT and final ferrite grain size. Samples were reheated to 1250°C for 5 min, air cooled to 675°C, held for 10 s and then deformed to strains of 0·8 and 2·0 at a strain rate of 3 s^{-1}. Samples were then either water quenched following deformation, or isothermally held at the deformation temperature for 10 s before quenching.

Effect of strain rate

This series of tests was conducted to study the effect of strain rate on the nucleation of intragranular ferrite during isothermal torsion testing. Samples were reheated to 1250°C, air cooled to 675°C and tested at strain rates of 0·3, 3, and 30 s^{-1} to a strain of 2·0, followed by water quenching.

Effect of cooling rate during deformation

In the preceding torsion tests, significant levels of supercooling were achieved by air cooling the large austenite grain sized samples down to isothermal deformation temperatures 100 – 150°C below the Ae_3 temperature. Of interest, however, is what effect accelerated cooling during torsion testing might have on the final microstructure compared to isothermally deformed samples. Previous work[13] involving rolling experiments on steel strip using a similar schedule to that used in this work have given rise to ultrafine ferrite grains at the surface of the strip. Roll chill of the strip by the large work rolls is believed to play an important part in the formation of the ultrafine ferrite grains. The present work enables this effect to be isolated.

Once the temperature of the specimen had reached 750°C, after air cooling from 1250°C, a process of simultaneous deformation at a strain rate of 3 s^{-1} (to a strain of 2·0) and water quenching of the specimen commenced. Quenching was continued for 3 s, followed by air cooling to room temperature. The final temperature of the specimen immediately following quenching was in the range 620 to 660°C, indicating that the average cooling rate during deformation was between 30 and 45° s^{-1}. The final microstructure was compared with that of a sample which was reheated to 1250°C for 5 min, air cooled to 675°C, deformed isothermally at a strain rate of 3 s^{-1} to a strain of 2·0, and then air cooled to room temperature.

Results

EFFECT OF DEFORMATION TEMPERATURE

Reflected light micrographs of the microstructures produced at the isothermal testing temperatures outlined above are presented in Fig. 1. The flow curves corresponding to each test are presented in Fig. 2.

At a deformation temperature of 825°C, no intragranular ferrite was formed during the test (Fig. 1*a*). This was expected, since the Ae_3 temperature of this steel was calculated to be 817°C. The corresponding flow curve (Fig. 2), therefore, represents the deformation of a purely austenitic microstructure. As expected, normal processes of work hardening were observed within the austenite during the test. However, the rate of work hardening approached zero towards the end of the test as the material began to dynamically recover/recrystallise.

At a deformation temperature of 750°C, a small amount of intragranular ferrite formed during deformation (Fig. 1*b*). As the deformation temperature was decreased to 725°C and 700°C, the amount of intragranular ferrite formed during the test increased (Fig. 1*c* and *d*). At 700°C, the amount of ferrite formed dynamically was sufficient to give rise to a decrease in the flow stress beyond a strain of $\sim$1·2 (Fig. 2). At a temperature of 675°C, extensive nucleation of intragranular ferrite had occurred during testing, giving rise to almost complete transformation of some austenite grains located in the surface of the deformed sample. Finally, examination of the microstructure of the specimen tested at 650°C revealed that very little intragranular polygonal ferrite had formed during this test (Fig. 1*f*). Instead, transformation to Widmanstätten ferrite occurred before or very early on in the test. This was presumably due to the low temperature of the test and the high effective level of undercooling which provided the driving force for this reaction. This form of ferrite presumably nucleated at the austenite grain boundaries and grew rapidly into the interior of the austenite grains. This ferrite morphology is known to give rise to a weak film on the austenite grain boundaries[19] and this probably led to premature failure of the specimen (Fig. 2) since strain localisation would have occurred in this softer phase.

Note that at all temperatures where DSIT of ferrite was observed, discrete ferrite grains formed into closely spaced parallel arrays or three dimensional 'rafts' of ferrite grains within each austenite grain. This is characteristic of the ferrite induced during the torsion process and arises due to the nature of the deformation defects produced within the austenite which most likely act as nucleation sites for the intragranular ferrite.[14] Ferrite grain size did not vary considerably over the temperature range in which it formed and was approximately 0·9 – 1·0 μm.

EFFECT OF STRAIN

Strain = 0·8 Figure 3*a* shows that ferrite had begun to nucleate within a few austenite grains near the surface of the sample, although the volume fraction of intragranular ferrite formed by this level of strain was small. Only a few austenite grains contained intragranular ferrite, with the most densely populated austenite grain containing a nucleation density of 0·19 – 0·21 grains μm^{-2} (in the two-dimensional cross-section measured). The ferrite grain size within this austenite grain was approximately $1{\cdot}33 \pm 0{\cdot}32$ μm, while the average aspect ratio of the ferrite grains was 2·41. This test was repeated with a 10 s isothermal dwell immediately after

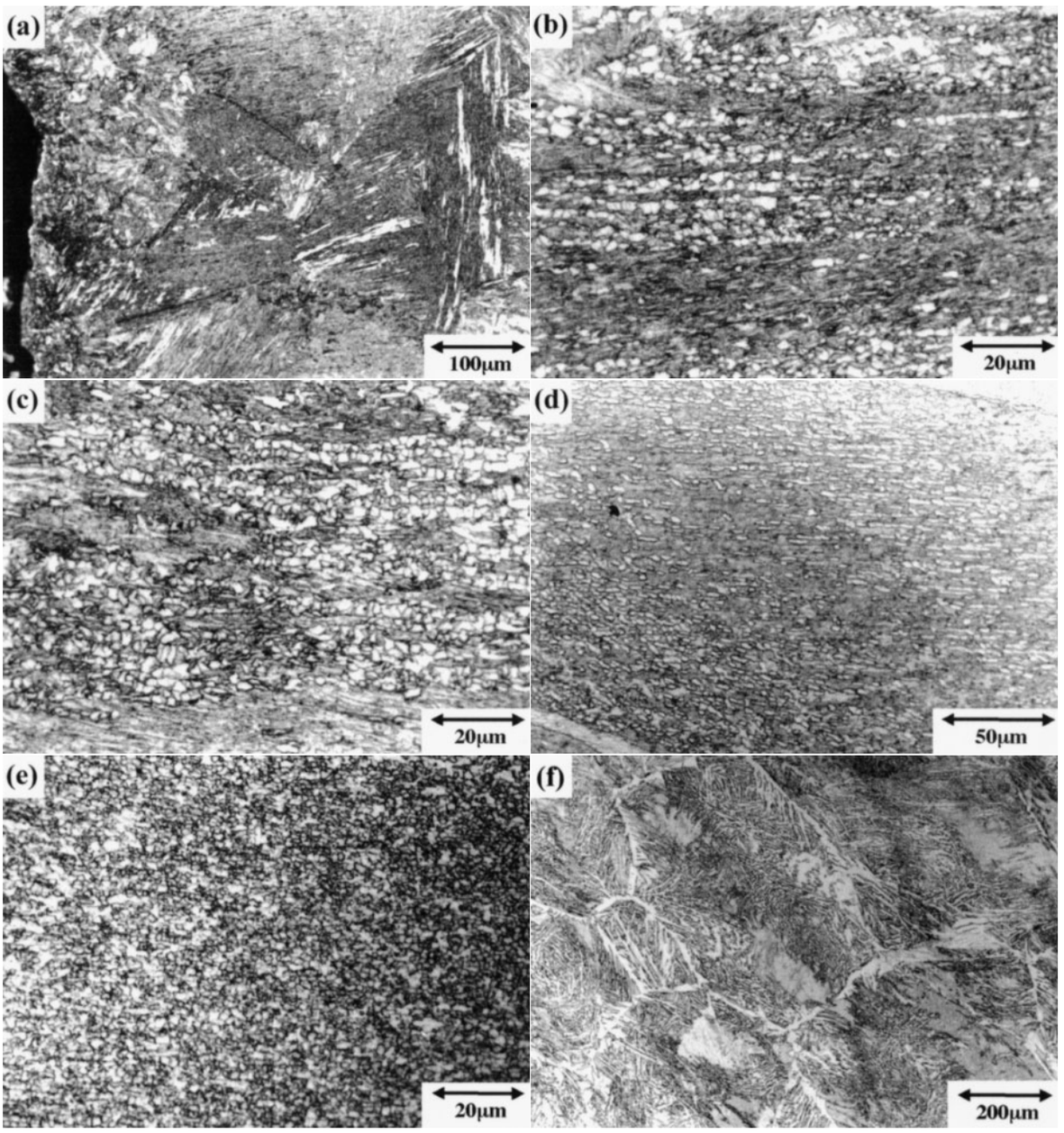

a 825°C; *b* 750°C; *c* 725°C; *d* 700°C; *e* 675°C; *f* 650°C

1 Reflected light micrographs of specimens deformed to applied strains of 2·0 at a strain rate of 3 s^{-1} at given temperatures

the deformation pulse and prior to water quenching. In this case, the ferrite grain size was discernibly larger (Fig. 3*b*) as a result of growth during the holding period. The average ferrite grain size was $4{\cdot}86 \pm 1{\cdot}24$ μm in the most densely populated austenite grain and the average aspect ratio of the ferrite was 3·64, indicating that ferrite growth occurred more rapidly along the direction parallel to the raft than normal to it. Growth probably occurs more rapidly in the plane of the raft than normal to it in response to diffusion rates that are higher along the planar arrays of defects that define the platforms for the ferrite rafts in the austenite. These rates might be expected to exceed those in regions remote from such defects (i.e. austenite regions between the ferrite rafts). The number density of intragranular ferrite grains observed after 10 s dwell was actually less than that in the water quenched sample, with the most densely populated austenite grain containing a number density of 0·028–0·036 grains μm^{-2}. This indicated that some ferrite grain coalescence may have occurred during the holding period.

Strain = 2·0 By a strain of 2·0, many austenite grains had almost completely transformed to ferrite, the ferrite grains having nucleated predominately within austenite grains during deformation (Fig. 4*a*). The average ferrite grain size within these grains was measured as $0{\cdot}91 \pm 0{\cdot}21$ μm, with an average aspect ratio of 2·1. Following a dwell of 10 s postdeformation (Fig. 4*b*), the average ferrite grain size was $1{\cdot}98 \pm 0{\cdot}36$ μm, with an aspect ratio of 2·09. The average number density of ferrite grains in the austenite was 0·27–0·35 grains μm^{-2}. Therefore, some coarsening had occurred but this was not specific to any given direction. It seems then, that as more

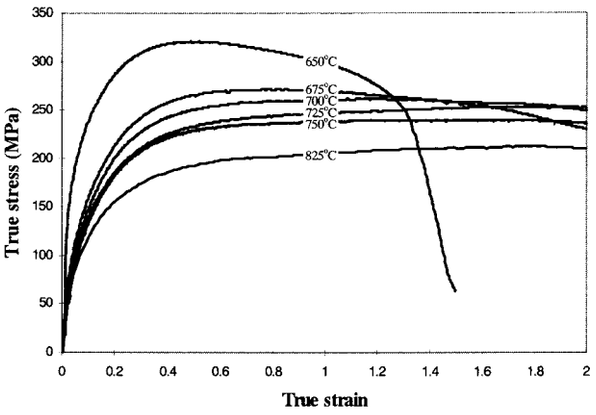

2 True stress–true strain curves obtained during torsion testing at different temperatures at a strain rate of 3 s^{-1}

grains were formed, impingement occurred within the planes of the rafts so that, on average, growth occurred more slowly within this plane as the strain is increased. At low strains, ferrite growth was more rapid within the raft plane, whereas at higher strains, ferrite growth was restricted within the raft plane due to early impingement between grains. Once impingement had occurred, growth presumably proceeded predominantly in the direction normal to the raft plane, decreasing the grain aspect ratio.

These results confirmed that the level of applied strain is of paramount importance for maximising the amount of dynamic strain induced ferrite during hot torsion testing. They also indicate that the final ferrite grain size is reduced when the applied strain is maximised. Also, it appears that inducing as much ferrite nucleation during deformation leads to a finer ferrite grain size than when ferrite forms once deformation has ceased. Once deformation has finished, the specimen should be quickly cooled to avoid growth.

EFFECT OF STRAIN RATE

For each of the three strain rates, similar trends in the flow curves were observed (Fig. 5) A peak in flow stress was observed at strain levels of 0·59, 0·74, and 0·77 for the strain rates of 0·3, 3, and 30 s^{-1} respectively. Beyond each peak, the flow stress decreased at an approximately steady rate until the completion of the test at a strain of 2·0.

The shape of the flow curves suggested that ferrite was formed during deformation at each of the strain rates tested, and microstructural examination confirmed that intragranular ferrite nucleation had occurred (Fig. 6*a*, 6*c*, and 6*e*). Furthermore, similar trends in the flow stress for the three strain rates suggested that similar amounts of ferrite formed at each strain rate, which was also qualitatively supported by the microstructures (Fig. 6*a*, 6*c*, and 6*e*).

Higher magnification imaging revealed (Fig. 6*b*, 6*d*, and 6*f*) that, for all strain rates, the ferrite nucleated in parallel rafts traversing individual austenite grains. There were, however, some noticeable differences in the morphology of

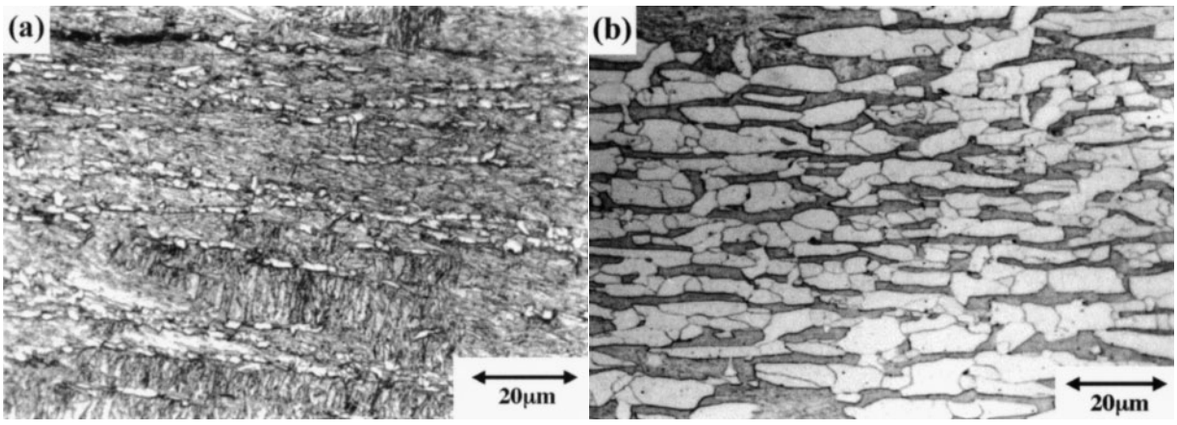

a water quenched; *b* held for 10 s after deformation then water quenched

3 Reflected light micrographs of specimens deformed to a strain of 0·8

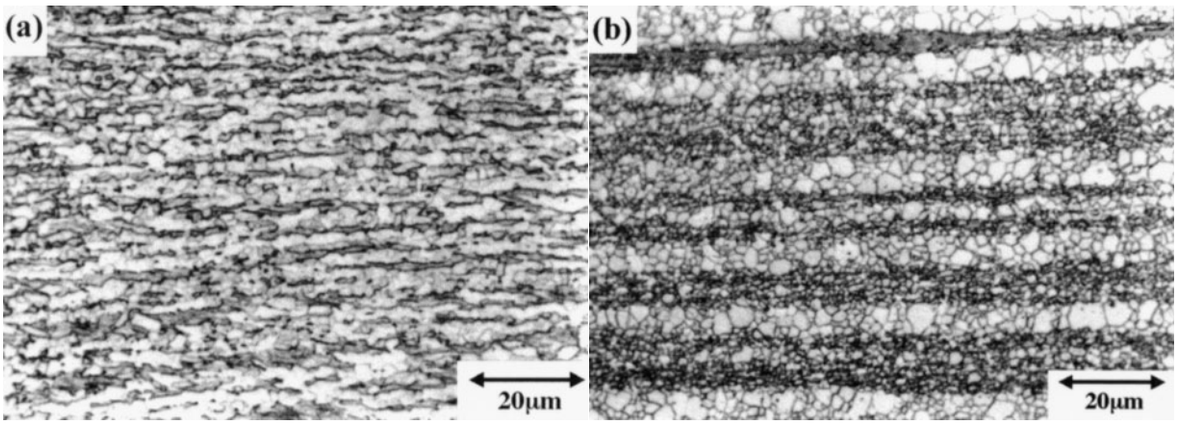

a water quenched; *b* held for 10 s after deformation then water quenched

4 Reflected light micrographs of specimens deformed to a strain of 2·0

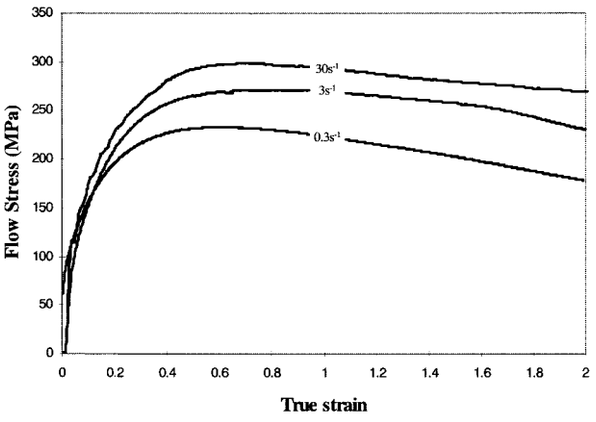

5 True stress–true strain curves obtained during torsion testing at different strain rates at 67°C

the ferrite nucleated at the three strain rates. For example, at a strain rate of 30 s^{-1} the ferrite that nucleated within the austenite was very fine after quenching (Fig. 6*a*). Also, the austenite contained mostly discrete ferrite grains with only minor growth or impingement of ferrite grains occurring before quenching. This is likely to be due to the rapid speed of this particular test. While the effective level of undercooling was equivalent at all three strain rates, the time between the start of the test and the final quench was extremely short for the specimen deformed at 30 s^{-1} (67 ms). The test conducted at a strain rate of 3 s^{-1} involved a period of 677 ms, while a deformation occurred over a period of 6770 ms for the slowest strain rate. In the very brief period of deformation at 30 s^{-1}, ferrite nucleated extensively within the austenite (Fig. 6*a*). However, there was very limited time for growth of the ferrite grains (Fig. 6*b*). The average ferrite grain size in the specimen

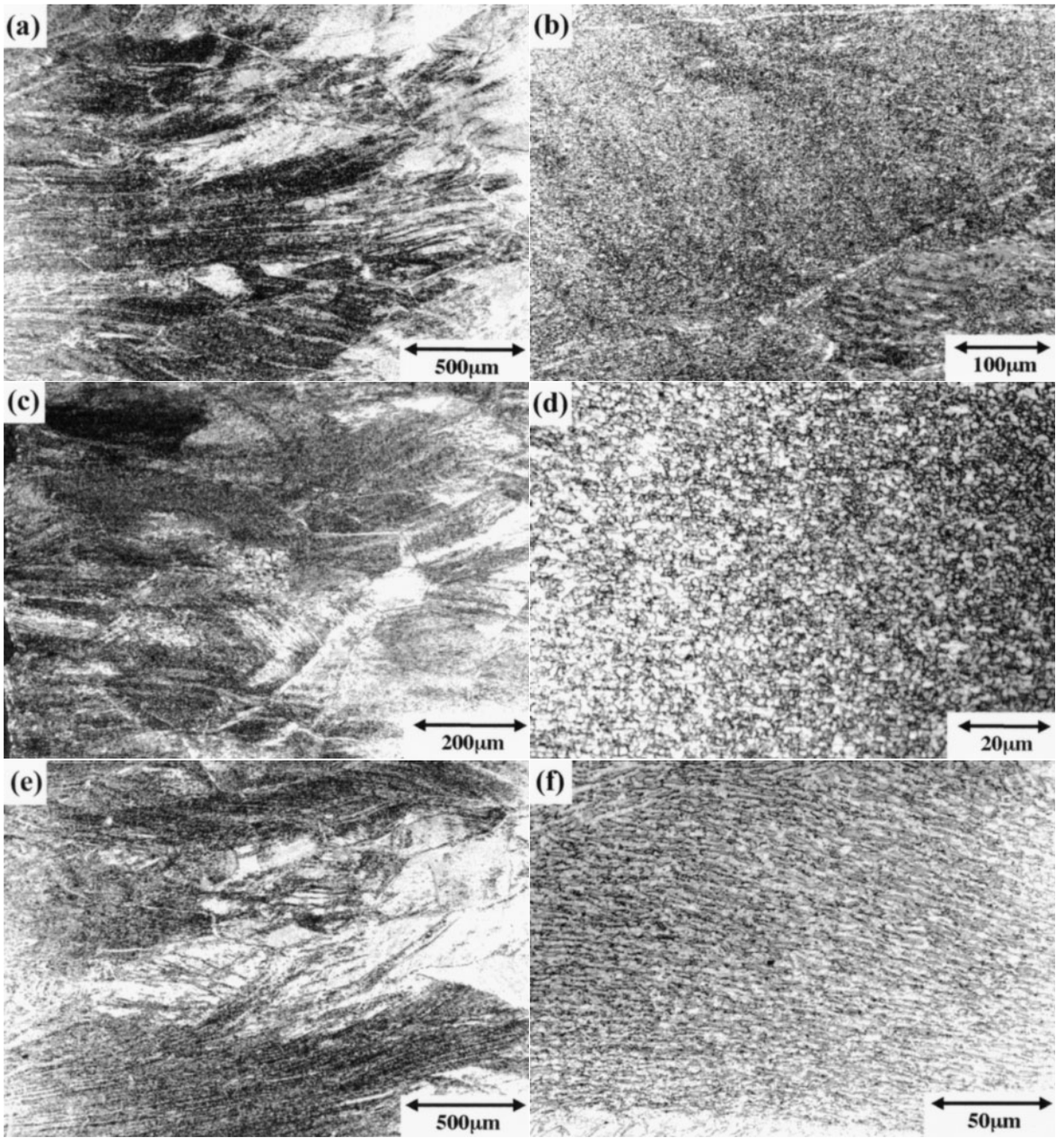

6 Reflected light micrographs of specimens deformed at 675°C to strain level of 2·0 at strain rates of *a,b* 30 s^{-1}; *c,d* 3 s^{-1}; *e,f* 0·3 s^{-1}

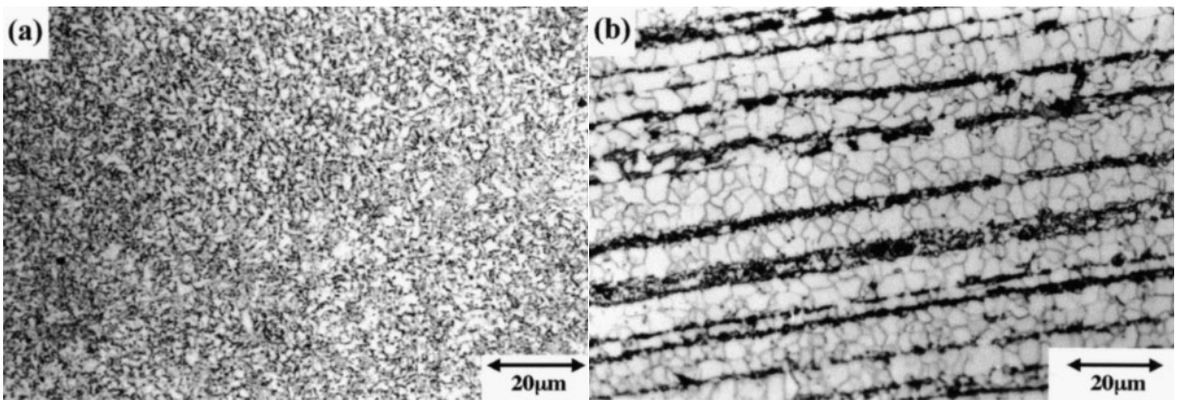

7 Reflected light micrographs of surface region of specimens deformed to applied strain of 2·0 and *a* simultaneously rapidly cooled from 750°C during deformation using water for 3 s; *b* isothermally deformed at 675°C and air cooled after testing

deformed at 30 s^{-1} was $0{\cdot}66 \pm 0{\cdot}13$ μm, with an average aspect ratio of 2·24.

In contrast, at the lowest strain rate of 0·3 s^{-1}, the ferrite nucleated during deformation coarsened considerably while deformation continued until the quench (Fig. 6*e* and *f*). The final microstructure consisted of continuous rafts of ferrite traversing austenite grains. The average ferrite grain size in this specimen was $1{\cdot}21 \pm 0{\cdot}35$ μm, while the average grain aspect ratio was 1·90. At lower strain rates, more grain growth occurs during deformation due to the increased time required to attain a given level of strain.

The microstructures of a specimen strained at 3 s^{-1} (Fig. 6*c* and *d*) were intermediate between those observed at the higher and lower strain rates (average ferrite grain size $0{\cdot}91 \pm 0{\cdot}21$ μm, average aspect ratio of 2·1). The ferrite had coarsened to some degree during the extended deformation period compared to a specimen deformed at 30 s^{-1}. However, grain growth and grain coalescence had not occurred to the same extent as in a specimen strained at 0·3 s^{-1}, again due to the shorter time at the deformation temperature.

This series of tests again highlights the importance of maximising the level of applied strain as quickly as possible followed by immediate cooling to prevent growth for reducing the final ferrite grain size.

EFFECT OF COOLING RATE DURING DEFORMATION

Figure 7*a* shows the microstructure of a specimen that was subjected to accelerated cooling from 750°C during torsion testing using the schedule described above. A very fine polygonal ferrite grain structure was achieved during this test; the average grain diameter was $0{\cdot}78 \pm 0{\cdot}11$ μm. The ferrite was observed to nucleate to form raft structures, and an important feature of the microstructure was the distribution and morphology of the carbide phase. Accelerated cooling led to a uniform dispersion of fine, spherical particles located on grain boundaries and triple junctions throughout the ferrite microstructure. Figure 7*b* shows the final microstructure of a specimen deformed isothermally at 675°C to an equivalent strain and air cooled following deformation. A final average ferrite grain size of $2{\cdot}21 \pm 0{\cdot}61$ μm was measured in this specimen. In this case, a finely spaced, banded carbide distribution exists throughout the ferrite microstructure. It is clear then that rapid cooling through the eutectoid temperature not only reduced the final ferrite grain size relative to a specimen air cooled through this temperature, but has also completely altered the dispersion of the second phase. The significance of this finding is discussed in the next section.

Discussion

DEFORMATION TEMPERATURE

It was shown above that lower deformation temperatures led to more extensive intragranular ferrite nucleation (Fig. 1*a*–*f*), presumably due to the higher effective supercooling of the austenite before ferrite formation. In Fig. 2 it was shown that a peak occurs in the stress–strain curve corresponding to a stage in the test where ferrite first begins to soften the material. The peak strains for each test temperature are plotted in Fig. 8 and clearly show how an increase in the level of undercooling leads to a systematic decrease in strain required to induced transformation during testing. This increased driving force allowed the activation energy barrier to ferrite nucleation in the steel to be overcome, and this appears to have given rise to a higher number density of ferrite nuclei during deformation. However, there is a lower limit to the isothermal deformation temperature possible, defined by the temperature at which Widmanstätten or bainite structures form before, or during, testing (Fig. 1*f*). Thus, a deformation temperature of 675°C was the most effective for producing extensive intragranular nucleation of ultrafine ferrite.

STRAIN LEVEL

The results showed that an increase in the number density of ferrite grains and a corresponding decrease in ferrite grain size within austenite grains occurred with increased strain.

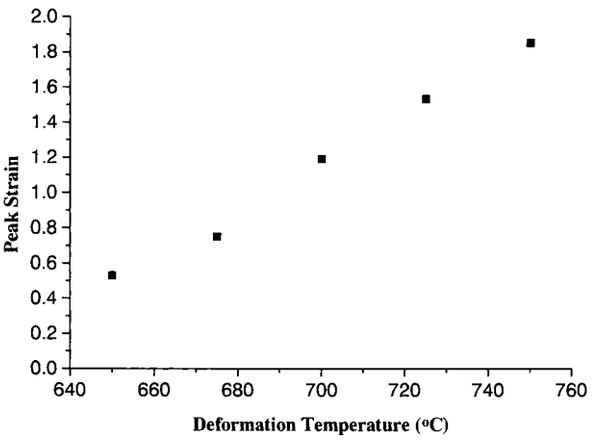

8 Peak strains measured for specimens tested at various isothermal deformation temperatures

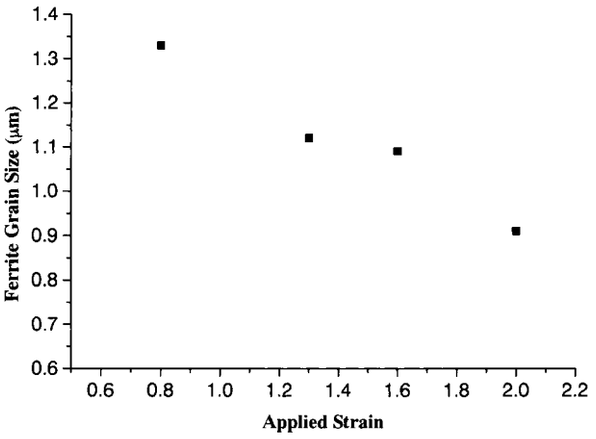

9 Measured ferrite grain sizes for specimens deformed to different levels of applied strain at 675°C at strain rate of 3 s^{-1}

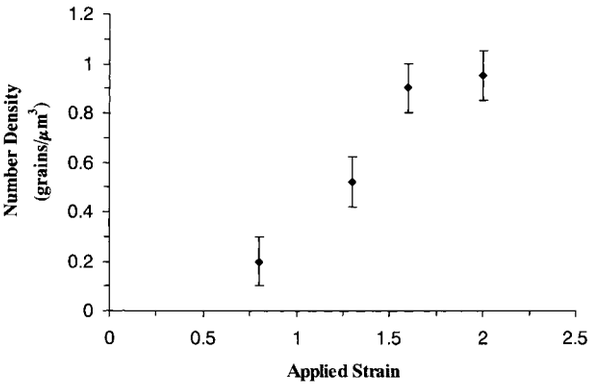

10 Measured ferrite number densities within grains for specimens deformed to different levels of applied strain at 675°C at strain rate of 3 s^{-1}

The ferrite grain size was slightly coarser in a specimen deformed to a strain of 0·8 and water quenched than that deformed to a strain of 2·0 and water quenched. This is possibly due to the extensive grain impingement that occurred in a deformed to the higher strain, which may have limited grain growth before the quench. A larger average grain size was measured for a specimen strained to 0·8 and held for 10 s (Fig. 3*b*) than that subjected to an equivalent isothermal dwell after a strain of 2·0 (Fig. 4*b*). This suggests that, as the strain increased, the density of potential nucleation sites for ferrite increased significantly as a result of further substructural development that occurred within the austenite. The ferrite nucleates preferentially on the defect structure formed during testing because the energy recovered through annihilation of the defects constitutes a net reduction in the energy barrier to nucleation. In earlier work,[20] the ferrite grain size and ferrite number fractions were determined for samples deformed to a strain level of 1·3 and 1·6 along with the results for samples deformed to levels of strain of 0·8 and 2·0 reported in the present work. These results are plotted in Fig. 9 and Fig. 10. Clearly, increasing the level of applied strain increases the density of nucleation sites within the austenite, which leads to a lower ferrite grain size. Although there appears to be an almost linear relationship between applied strain and ferrite grain size in Fig. 9 up to the point of maximum strain applied in this work, it is reasonable to assume that the grain size would be expected to asymptote towards a limiting value as nucleation site saturation occurred at higher levels of strain.

STRAIN RATE

Strain rate appeared to have little effect on the characteristics of the nucleation sites or the density of such sites. The ferrite grains were observed to nucleate at all strain rates tested (in the range from 0·3 to 30 s^{-1}) in closely spaced parallel rafts within the large austenite grains, with similar volume fractions of ferrite for a given level of strain (Fig. 6) However, differences existed in ferrite morphology after testing at different strain rates. At the highest strain rate of 30 s^{-1}, the average ferrite grain size after an applied strain of 2·0 was very fine (0·66$\pm$0·13 μm) and the ferrite was observed to be form as discrete grains apparently along planar defect arrays in the austenite. As the strain rate decreased, the ferrite formed by a strain of 2·0 had more time to coarsen during deformation. Therefore, the grain size was coarser for any given level of applied strain, and at a strain rate of 0·3 s^{-1} the final microstructure consisted of ferrite with a larger average grain size (1·21$\pm$0·35 μm). For samples tested at low strain rates, some ferrite grains had undergone significant deformation during the test, giving rise to recovery and polygonisation to form many fine subgrains within each grain (Fig. 6*f*). Note that, even after deformation to a strain of 2·0 at a strain rate of 0·3 s^{-1}, in which deformation took over 6 s to complete, very little ferrite was observed in the regions between the ferrite rafts (Fig. 6*f*). Instead, the ferrite rafts were separated by regions of martensite produced during the quench. The absence of any ferrite in these regions at each strain rate shows that the austenite in these regions remained metastable for extended periods at this temperature. This highlights the significant decrease to the energy barrier to ferrite nucleation on the planar defects introduced into the austenite by deformation relative to regions away from the planar defects. These planar defects have been shown to be microbands, with the regions separating them remaining relatively low in dislocation density.[14] The fact that similar volume fractions of ferrite formed during testing at each strain rate suggests that the nature of the microbands formed at the three strain rates studied is similar and that the potency of the microbands for acting as ferrite nucleation sites is not affected by strain rate.

ACCELERATED COOLING

It is demonstrated above that accelerated cooling of a sample from 750°C to 640$\pm$20°C (cooling rate of 30 to 45° s^{-1}) during the deformation at a strain rate of 3 s^{-1} to a strain of 2·0, followed by air cooling to room temperature, led to a finer average ferrite grain size (0·78$\pm$0·11 μm) than was observed when this steel was deformed isothermally at 675°C, using the same strain and strain rate, and water quenched to room temperature (average ferrite grain size of 0·91$\pm$0·21 μm). Although the difference is barely significant, it is sufficient to suggest that perhaps the ferrite nucleation density was higher when the steel was rapidly cooled during deformation, presumably due to the higher effective undercooling achieved in the later stage of deformation when accelerated cooling was applied. Furthermore, it may be that the growth rate of the ferrite during deformation was also reduced when the steel was rapidly cooled during the test, again due to the lower temperature of the specimen in the later stages of deformation. Accelerated cooling (postdeformation) of low carbon steels has been found to increase the volume fraction of intragranular ferrite formed compared to when air cooling follows deformation.[21] This has been attributed to the increase in undercooling which accelerated cooling sustains, as well as to a decrease in growth rate of ferrite grains already nucleated.[21] The present work has shown that a similar situation may also hold when rapid cooling rates are used

during a process giving rise to dynamic strain induced transformation of intragranular ferrite.

The average final ferrite grain size in the rapidly cooled sample was also considerably finer than that in the sample which was deformed isothermally at 675°C at a strain rate of 3 s^{-1} to a strain of 2·0 and then air cooled to room temperature (average ferrite grain size of $2{\cdot}21 \pm 0{\cdot}61$ μm). This suggests that the growth rate of the ferrite in the sample subjected to accelerated cooling during deformation was reduced significantly once deformation had ceased. This may be due to the distribution and morphology of the carbide phase which formed in the rapidly cooled sample, and which consisted of fine spherical particles situated primarily at grain boundaries and triple point junctions of the ferrite grains (Fig. 7*a*). These carbide particles could be responsible for pinning grain boundaries and restricting growth during air cooling. In the sample that was deformed isothermally and then air cooled to room temperature, the microstructure consisted of a banded distribution of carbide phase (Fig. 7*b*). In this case, the carbide was not distributed uniformly across the microstructure at many ferrite grain boundary regions, as it was in the sample which was rapidly cooled during deformation. Thus, the carbide phase in the sample deformed isothermally would be less effective at restricting the migration of ferrite grain boundaries. When air cooling is applied following deformation, the ferrite grains formed during the test are able to grow and impinge on one another, leading to partitioning of the solute carbon into the surrounding austenite. During the final stages of transformation, pearlite forms in these regions of solute rich austenite. Accelerated cooling restricts the partitioning of solute leading instead to large scale precipitation of fine carbide particles.

The microstructure in the sample quenched during deformation is remarkably similar to the microstructure observed in the surface layer of strip rolled using a recently reported rolling process,[12,13] which also consisted of a dispersion of fine spherical carbide particles located on the grain boundaries and triple point junctions of an ultrafine equiaxed ferrite microstructure. The inference can be made that the accelerated cooling brought about by roll chill in the strip rolling process was responsible not only for providing the high driving force for ferrite nucleation, but also for modifying the morphology and distribution of the carbide phase. Moreover, it is possible, given the results from the present work, that the carbide phase formed in the surface of the steel strip was responsible, at least to some extent, for restricting grain growth during air cooling after rolling.

Conclusions

Hot torsion was used to study the effect of isothermal deformation temperature, strain level, strain rate and cooling rate during deformation on the efficiency of ferrite grain refinement resulting from dynamic strain induced transformation in a hot worked 0·11C–1·68Mn–0·2Si (wt-%) steel. The following were found.

1. Decreasing the deformation temperature increased the amount of dynamic straininduced ferrite. This is due to the increased driving force resulting from the higher level of undercooling at lower temperatures. If the test temperature was too low, Widmanstätten ferrite formed during the test, leading to premature failure of the specimen. The optimum temperature for inducing dynamic intragranular ferrite was 675°C for the steel used in this work. Dynamic strain induced ferrite was produced at temperatures as high as 750°C for this steel.

2. The amount of intragranular ferrite increased as a direct result of the applied strain. At a strain of 0·8, ferrite had begun to nucleate intragranularly in the austenite at 675°C. By a strain of 2·0, many austenite grains at the surface of the torsion specimens had almost completely transformed to ferrite via the process of intragranular ferrite nucleation and growth.

3. The process of dynamic strain induced transformation to ferrite appeared to be independent of strain rate. When tested at strain rates of 30, 3, and 0·3 s^{-1} at 675°C, ferrite grains formed in parallel raft like structures within the austenite. Moreover, the number density of ferrite grains was similar at each strain rate, indicating that strain rate had little effect on the nucleation sites in the austenite. As the strain rate was decreased from 30 to 3 and then to 0·3 s^{-1}, the tendency for the strain induced ferrite to undergo polygonisation and form subgrains increased. This was attributed to the increased deformation time resulting from the slower strain rates, which enabled the ferrite that formed at lower strains to undergo recovery.

4. Very fine ferrite grain sizes were achieved when accelerated cooling accompanied the dynamic strain induced transformation of ferrite during torsion testing. Rapid cooling also modified the carbide phase. Instead of the banded carbide structure formed during air cooling, discrete carbide particles were observed to be located at ferrite grain boundaries and triple junctions in the ferrite microstructure.

Acknowledgements

One author (PJH) wishes to thank the Australian Government and BHP Research for funding during the course of this work. The other author (PDH) would like to acknowledge the financial support of the Australian Research Council. The authors would like to thank Professor B. C. Muddle for helpful discussions.

References

1. G. B. OLSON: 'Encyclopedia of materials science and engineering', 2929–2931; 1985, Oxford, Pergamon.
2. R. PRIESTNER and L. ALI: *Mater. Sci. Technol.*, 1993, **9**, 135–141.
3. R. PRIESTNER and E. DE LOS RIOS: *Met. Technol.*, 1980, **7**, 309–316.
4. R. PRIESTNER: 'Thermomechanical processing of austenite', (ed. A. J. DeArdo *et al.*), 455–466; 1982, Warrendale, PA, TMS.
5. R. K. AMIN and F. B. PICKERING: 'Thermomechanical processing of microalloyed austenite', (ed. A. J. DeArdo *et al.*), 377–403; 1982, Warrendale, PA, TMS.
6. H. YADA, Y. MATSUMURA, and K. NAKAJIMA: Nippon Steel Corp.; 'Ferritic steel having ultra-fine grains and a method for producing the same', Japanese Patent 4466842, Tokyo, 1984.
7. Y. MATSUMURA and H. YADA: *Trans. ISIJ*, 1987, **27**, 492–498.
8. H. YADA, Y. MATSUMURA, and T. SENUMA: Proc. Int. Conf. on 'Martensitic transformations', ICOMAT 86, Nara, Japan, August 1986, Japan Institute of Metals, 515–520.
9. H. YADA, Y. MATSUMURA, and T. SENUMA: Proc. Int. Conf. on 'Physical metallurgy of thermomechanical processing of steels and other metals', Thermec '88, (ed. I. Tamura), Tokyo, Japan, June 1988, Iron and Steel Institute of Japan, 200–207.
10. L. SUNGHAK, K. DONGIL, K. L. YOUNG, and K. OHJOON: *Metall. Mater. Trans. A*, 1995, **26A**, 1093–1100.
11. J. H. BEYNON, R. GLOSS, and P. D. HODGSON: *Mater. Forum*, 1992, **16**, 37–42.
12. P. D. HODGSON, M. R. HICKSON, and R. K. GIBBS: *Scr. Mater.*, 1999, **40**, 1179–1184.
13. P. J. HURLEY, P. D. HODGSON, and B. C. MUDDLE: *Scr. Mater.*, 1999, **40**, (4), 433–438.
14. P. J. HURLEY, B. C. MUDDLE, P. D. HODGSON, C. H. J. DAVIES, B. P. WYNNE, P. CIZEK, and M. R. HICKSON: *Mater. Sci. Forum*, 1998, **284–286**, 159–166.
15. J. S. KIRKALDY, B. A. THOMSON, and E. A. BAGANIS: 'Hardenability concept with applications to steels', (ed. D. V. Doan and J. S. Kirkaldy), 82–125; 1978, Warrendale, PA, AIME.

16. H. WEISS, D. H. SKINNER, and J. R. EVERETT: *J. Phys. E: Sci. Instrum.*, 1973, **6**, 709–714.
17. D. S. FIELDS and W. A. BACKOFEN: *ASTM Proc.*, 1957, **57**, 1259–1272.
18. P. D. HODGSON: 'Mathematical modelling of recrystallisation processes during the hot rolling of steel', PhD thesis, Univerisity of Queensland, Brisbane, Australia, 1992.
19. J. R. YANG and L. C. CHANG: *Mater. Sci. Eng. A*, 1997, **A223**, 158–167.
20. P. J. HURLEY: 'Production of ultra-fine ferrite during thermo-mechanical processing of steels', PhD thesis, Monash University, Melbourne, Australia, 1999.
21. T. ABE, K. TSUKADA, and I. KOZASU: *Tetsu to Hagané*, 1988, **74**, 505–512.